Proceedings of the 2003 IEEE/RSJ
Intl. Conference on Intelligent Robots and Systems
Las Vegas, Nevada · October 20033

Realtime ZMP Compensation for Biped Walking Robot using Adaptive Inertia Force Control

Yu Okumura, Tetsuo Tawara, Ken Endo, Takayuki Furuta and Masaharu Shimizu

Future Robotics Technology Center, Chiba Institute of Technology

Abstract— **A method of stabilizing the biped locomotion in real-time is necessary to achieve biped locomotion that is stable and practical. We propose a new walk stabilization technique. First, we define the ZMP stability index. The proposed method compensate ZMP in real-time to control of inertia force and adjust feedback parameters according to the stability index. This results in altering the speed of walk instead of the walk pattern. As a result, we can compensate ZMP without changing the walking pattern and achieve both of the robustness against disturbances and high responsiveness for ZMP error correction. In this paper, after describing the proposed real-time ZMP compensation method, the validity of the proposed method are tested using humanoid robot named 'morph3' that is created in our laboratory. Verification experiments, including simulation are performed and their results prove the validity of the proposed method.**

I. INTRODUCTION

Humanoid based research has become a hot topic in recent years [5][6][7][11]. Because of it's form, humanoid robots can adapt to the human work environment without major changes to the infrastructure. Therefore, it is ideal for domestic support use and work in hazardous environments. In order for humanoid robots to succeed in the real world, stable bipedal locomotion is a necessity. Humanoid robots are especially susceptible to toppling over. To achieve practical and stable biped locomotion, the following two problems have to be solved. First, it is commonly done to adjust joint angles in order to compensate ZMP error. However, this introduces modification of the walking pattern that is designed a priori. This may not be desirable because landing points of the free leg will be altered and may touch down at unwanted positions. This problem is more prevalent on irregular surface like steps. A new algorithm for adaptive ZMP compensation controller that utilizes inertial loading and preserves footprints of biped walking is proposed in this paper. To achieve ZMP compensation performance both the stability and high responsibility, the following two new technologies are introduced. First technology is a ZMP compensation algorithm based on a unique idea that an acceleration $\ddot{X}$ acting on a mass M induces an inertial loading of $M \cdot \ddot{X}$ along the opposite direction of the acceleration.

Here, this fact is advantageously used in ZMP compensation where the position of ZMP is shifted by a tactically chosen inertial loading. A fact that needs to be considered here is that the acceleration acted on a robot causes shifts in its center of gravity and this induces shifts of the landing positions of the swinging leg. This may not be desirable since the landing position is normally determined according to exogenous environmental needs. The proposed algorithm has a unique feature that preserves pre-assigned landing positions of the swinging leg.

In this paper, after describing the proposed real-time ZMP compensation method, the validity of the proposed method are tested using humanoid robot named 'morph3' that is created in our laboratory. Verification experiments, including simulation are performed and their results prove the validity of the proposed method.

II. ZMP COMPENSATION FUNCTION

A. Planar Models for Control

The motion of biped robots is generated by synchronizing two planar motion. Models in these two planes called sagittal and lateral plane are shown in Fig. 1. The origin of the absolute coordinate system coincides with the ankle joint of the supporting leg.

To realize stable walk, it is needed that the foot of the supporting leg is stationary on the ground during the motion in each step. This condition is exceedingly essential not only to simplify the dynamic equations but also to meet the gait stability. To assume that the foot of supporting leg is fixed on the ground, the following conditions must be satisfied during each step. 1) The positions of the foot in vertical and horizontal directions must be fixedly maintained. 2) The direction angle of the foot must be fixedly maintained. The first condition is neglected without the loss of the influence to the gait stability. The walking motion is performed within the vicinity of the vertical axis so that the external force to the foot in the vertical direction is approximately the value related to the gravity acceleration of the total mass of the robots. The horizontal friction force is enough to fix the supporting foot because we can equip the bottom of the foot with a material that has a large friction coefficient such as a rubber sheet. The second condition related to the rotation of the foot is significant for stable walking. This condition can be stated as the following ZMP criterion: the zero moment point(ZMP) of a biped

0-7803-7860-1/03/$17.00 © 2003 IEEE

robot is sustained within the supporting surface, or the foot of the supporting leg in the single-leg supporting phase. ZMP can be represented as follows,

$$X_{zmp} = \frac{\sum_{i=1}^{n} x_i m_i(\ddot{z}_i + g) - \sum_{i=1}^{n} m_i \ddot{x}_i z_i}{\sum_{i=1}^{n} m_i(\ddot{z}_i + g)} \cong -\frac{\tau_{s1}}{Mg} \quad (1)$$

$$Y_{zmp} = \frac{\sum_{i=1}^{n} y_i m_i(\ddot{z}_i + g) - \sum_{i=1}^{n} m_i \ddot{y}_i z_i}{\sum_{i=1}^{n} m_i(\ddot{z}_i + g)} \cong -\frac{\tau_{l1}}{Mg} \quad (2)$$

where m_i are masses of link-i, x_i, y_i and z_i are positions of the masses of link-i and M is the mass of the biped robot. From this equation, the ZMP criterion reduces to a condition on the ankle joint torque τ_{s1} and τ_{l1} that τ_{s1} and τ_{l1} be small enough so that the above ZMP lies within the foot print.

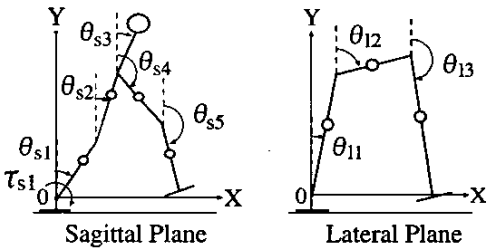

Fig. 1. Biped Models in Two Planes

B. Overview of the ZMP Compensation Strategy

The proposed algorithm has a unique feature that preserves the pre-assigned landing positions of the swinging leg. Since the contact point of the leg will not change during compensation, it is possible to use for difficult terrain, such as walking on stepping stones, or on staircases, which have little margin for corrections. The proposed algorithm is based on a simple principle that an acceleration $\ddot{X}_G$ acting on a mass M induces an inertial loading of $M\ddot{X}_G$ along the opposite direction of the acceleration. This is used as an advantage in ZMP compensation where the position of ZMP is shifted by a tactically chosen inertial loading. A fact that needs to be considered here is that the acceleration acted on a robot causes shifts in its center of gravity and this induces shifts of the landing positions of the swinging leg. This may not be desirable since the landing position is normally determined according to exogenous environmental needs.

The main idea of the proposed algorithm is the virtual shift of sampling intervals on a real-time basis. A simple observation is that the same spatial trajectory in 3D (Fig. 2) can be traversed at different speeds and that the difference in speed is nothing but the difference in sampling time. The change of temporal trajectory of an angle that corresponds to two different sampling intervals is depicted in Fig. 3. Obviously different acceleration is needed for the two trajectories in Fig. 3. Conversely, if an extra acceleration is exerted on a robot in such a way that the relationship between Fig. 2 and Fig. 3 is satisfied, then the resulting spatial trajectory will not be disturbed. Thus, a conclusion is derived that the acceleration that is required for ZMP compensation can be exerted without disturbing the pre-computed spatial trajectory. It is mentioned that there are obvious limits in applicable acceleration. This limit becomes more visible when we derive a relationship between the ZMP compensating acceleration and the deviation in sampling interval. First, we introduce the structure of the proposed compensator and discuss the role of each component.

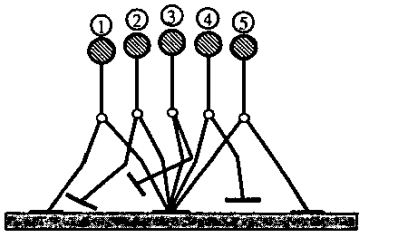

Fig. 2. Stick Diagram of Robot in Sagittal Plane

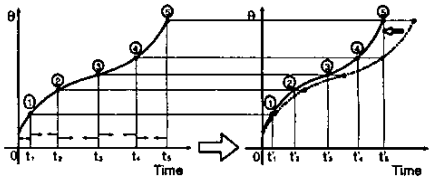

Fig. 3. Relationship between Tc and Angle Trajectory

C. Structure of the proposed ZMP compensator

The structure of the proposed ZMP compensator with inertial loading is shown in Fig. 4. The processing by the ZMP compensator is explained using this figure.

The temporal trajectory θ_{ref} computed by the gait generator is transformed to the ZMP position ZMP_{ref} by the ZMP Transfer Function. The obtained ZMP_{ref} is compared with the actual ZMP measured by a ZMP sensor and the error ZMP_{err} between them is fed to the ZMP Compensator. This error and the ZMP_{ref} are first used by ZMP Virtual Reference Generator to compute a quantity called the virtual reference ZMP: ZMP_{vref} that indicates (1) possibility of compensation and (2) amount

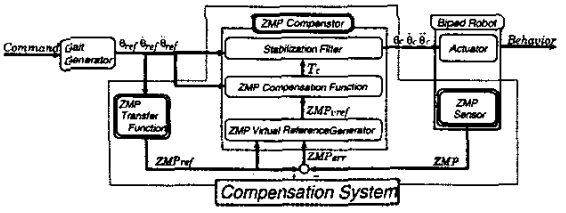

Fig. 4. Block Diagram of ZMP Compensation system

of compensation if compensation is possible. We introduce the stability index J_{cost} given by the following equation.

$$J_{cost} = Gain_1 \times \sum ZMP_{err}{}^2 + Gain_2 \times V^2 \qquad (3)$$

where, the design parameters $Gain_1$ and $Gain_2$ are positive number and V denotes the walking speed. Now, we define ZMP_{vref} as the following:

$$ZMP_{vref} = ZMP_{ref} + J_{cost} \times ZMP_{error} \qquad (4)$$

Using (4), ZMP_{vref} can be decided adaptively.

Then, the heart of computation, that is, the computation of new sampling interval T_c is performed by the ZMP Compensation Function from ZMP_{vref} and the reference temporal trajectory θ_{ref}. Finally, this T_c and the temporal reference trajectory are used by the Stabilizing Filter to compute the next reference angle θ_c at physical sampling instants that are unchanged due to external and/or hardware configuration.

D. ZMP Compensation Function

In this subsection, The compensation function is discussed. Now, We start our analysis with a sagittal plane model of a walking robot shown in Fig.1. The function is derived from (1) and (2).

First, we set the following equations:

$$\ddot{\theta}_{k+1} = \frac{\dot{\theta}_{k+1} - \dot{\theta}_k}{T_c}, \dot{\theta}_{k+1} = \frac{\theta_{k+1} - \theta_k}{T_c}, \dot{\theta}_k = \frac{\theta_k - \theta_{k-1}}{T_{c-old}}$$

then, A'_x and A'_z are defined as the following:

$$A_{xi} = V_{x1}\frac{1}{T_c^2} - W_{xi}\frac{1}{T_{c-old}}\frac{1}{T_c}$$
$$A_{zi} = V_{z1}\frac{1}{T_c^2} - W_{zi}\frac{1}{T_{c-old}}\frac{1}{T_c}$$

where

$$\begin{aligned}
V_{xi} &= \{\theta_{i(k+1)} - \theta_{i(k)})\}cos\theta_{i(k+1)} \\
&\quad -\{\theta^2_{i(k+1)} + \theta^2_{i(k)} - 2\theta_{i(k+1)}\theta_{i(k)}\}sin\theta_{i(k+1)} \\
V_{zi} &= \{\theta_{i(k+1)} - \theta_{i(k)})\}sin\theta_{i(k+1)} \\
&\quad -\{\theta^2_{i(k+1)} + \theta^2_{i(k)} - 2\theta_{i(k+1)}\theta_{i(k)}\}cos\theta_{i(k+1)} \\
W_{xi} &= \{\theta_{i(k)} - \theta_{i(k-1)}\}cos\theta_{i(k+1)} \\
W_{zi} &= \{\theta_{i(k)} - \theta_{i(k-1)}\}sin\theta_{i(k+1)}
\end{aligned}$$

Using these terms, (1) can be computed as the following:

$$\begin{aligned}
X_{zmp} &= \frac{\alpha_x A_{z1} + \beta_x A_{z2} + \gamma_x A_{z4} + \delta_x A_{z5} + \varepsilon_x}{\alpha A_{z1} + \beta A_{z2} + \gamma A_{z4} + \delta A_{z5} + \varepsilon} \\
&\quad - \frac{\alpha_z A_{x1} + \beta_z A_{x2} + \gamma_z A_{x4} + \delta_z A_{x5}}{\alpha A_{z1} + \beta A_{z2} + \gamma A_{z4} + \delta A_{z5} + \varepsilon}
\end{aligned} \qquad (5)$$

Other terms can similarly be computed and expressed as follows:

$$\begin{aligned}
\kappa &= (\alpha_x - \alpha X_{zmp})V_{z1} + (\beta_x - \beta X_{zmp})V_{z2} \\
&\quad +(\gamma_x - \gamma X_{zmp})V_{z4} + (\delta_x - \delta X_{zmp})V_{z5} \\
&\quad -\alpha_z V_{x1} - \beta_z V_{x2} - \gamma_z V_{x4} - \delta_z V_{x5} \\
\lambda &= (\alpha_x - \alpha X_{zmp})W_{z1} + (\beta_x - \beta X_{zmp})W_{z2} \\
&\quad +(\gamma_x - \gamma X_{zmp})W_{z4} + (\delta_x - \delta X_{zmp})W_{z5} \\
&\quad -\alpha_z W_{x1} - \beta_z W_{x2} - \gamma_z W_{x4} - \delta_z W_{x5} \\
\mu &= \varepsilon_x - \varepsilon X_{zmp}
\end{aligned}$$

Using those in (5), we obtain

$$\kappa = \frac{1}{T_c^2} - \lambda\frac{1}{T_{c-old}}\cdot\frac{1}{T_c} + \mu \qquad (6)$$

Finally, by solving (6) for time t, we obtain the following expression that is the compensation function.

$$T_c = \frac{2\kappa T_{c-old}}{\lambda \pm \sqrt{\lambda^2 - 4\kappa\mu T^2_{c-old}}} \qquad (7)$$

It is noted that the compensation function for the lateral plane dynamics can be obtained similarly.

III. HARDWARE PLATFORM: 'MORPH3'

A new humanoid robot has been developed to implement our theories. View of compact humanoid morph3 is shown in Fig. 5. Specifications of morph2 are shown in Table I

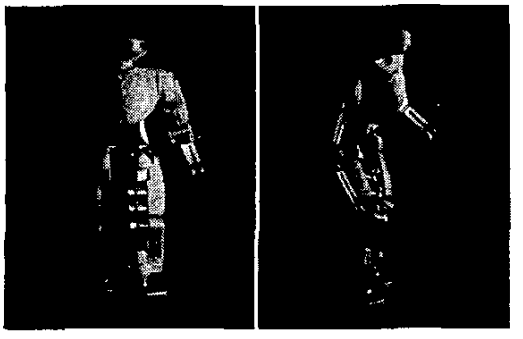

Fig. 5. View of Humanoid morph3 (Photo by Yukio Shimizu)

TABLE I
SPECIFICATIONS OF CONSTRUCTED MORPH3

Dimension[mm]	380
Mass[kg]	2.4
DOFs	Total:30 eyes :1/eys Head: 2 Legs: 6/leg Arm : 6/arm Waist: 2
Sensors	138 Sensors
Main Material	Duralmin
Other equipments	Bluetooth Module

morph3 is 380[mm] in height and 2.4[kg] in weight with a battery. Duralumin is used as the major construction material for the body of robot. morph3 has 30 DOFs, which are 6 DOFs in leg, 2 DOFs in waist, 6 DOFs in arm with 1 DOF in hand, 4 DOFs in head with 2 DOFs in eye.

a lot of sensors compared with other morph series are implemented in morph3. That is to say, morph 3 is equipped with ten types of sensors in the compact body and amount of these sensors is one hundred therty eight. In details, they are the followings:

1) two CCD cameras in the head
2) thirty four rotary position sensors all joints
3) twenty four force sensors in both feet
4) eighteen thermal sensors on large motors
5) eight contact force sensors on both elbows and knees, the back, and the hip
6) three gyros in waist
7) fifteen accelerometers in both arms and legs and the waist
8) thirty one current sensors on almost all motors
9) one terrestrial magnetism sensor in the body
10) one voltage sensor in the body
11) one infrared sensor in the neck
12) two CMOS cameras in the head

The electronic configuration of morph is shown in Fig.6. There are problems to manage a lot of sensor data with only one device. Therefore, we adopt a network framework called On-Body-Network that is formed by connection of multiple " small " processing devices and a powerful processing device. " Small " means literally small size and limited functions. The small processing device has several ADC ports and I/O ports . These devices are distributed on the whole body of the humanoid. The robot's behavior and decision generation process is executed the onboard powerful main CPU module. Numerous satellite CPU modules control the actuators and sensor devices independently. The main CPU module and the satellite CPUs are connected via on body LAN. Using this distributed CPU system, sensor data from one hundred thirty eight sensors can be gathered by the network of fourteen small processing devices. There is also a bluetooth communication module, which is used to send commands and receive data from the robot. With this configuration, the robot is capable of operating as a complete autonomous entity, with the batteries supplying power for an average of 30 minutes.

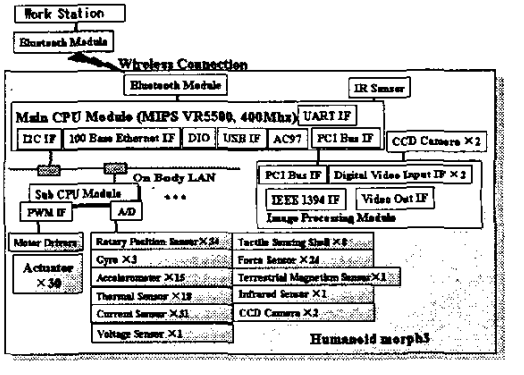

Fig. 6. Electronics Configuration of morph3

IV. VERIFICATION EXPERIMENTS

Viability of the ZMP compensation is first checked by performing a simulation. Then, the method is implemented onto our newly constructed humanoid robot and tested.

A. Simulation

In simulation, characteristic values of our biped robot Morph are used. The assumed motion is the stamping motion that requires Lateral gait only and is easy to generate and to check effects of the proposed method. The duration of a single-leg supporting phase in the generated gait is 0.7 sec. A disturbance in ZMP position

is introduced at 0.42 sec mark from the start of a single-leg supporting phase. First, reference and actual ZMP trajectories are plotted in Fig. 7 where the vicinity of ZMP disturbance depicted by dotted square is enlarged in Fig. 8.

Figure 8 shows the performance of the proposeed control method.

B. Implementation onto morph3

The scenario of the experiment is the same as that of the simulation. A push from the side of the robot is used as the cause for the ZMP disturbance. A set of typical results with and without the compensator is plotted in Fig. 9. It can be seen that the compensated ZMP trajectory is closer to the ZMP_{ref} generated from the reference gait.

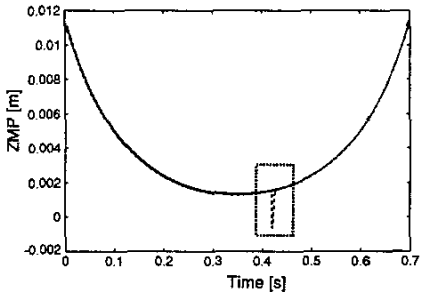

Fig. 7. ZMP Trajectory of Simulation

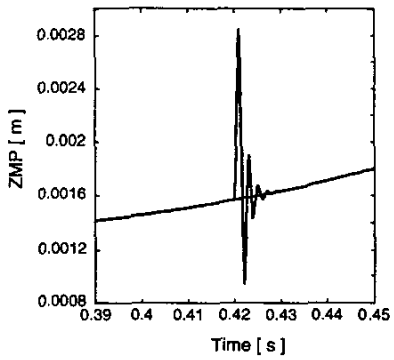

Fig. 8. ZMP Trajectory of Simulation (Enlarged)

V. CONCLUSIONS

A real-time ZMP compensation method using adaptive inertia force compensation has been presented. The proposed controller is implemented on a new humanoid robot 'morph3', which we developed as a research platform. The result of experiments shows the performance of the controller and prove the validity of the method

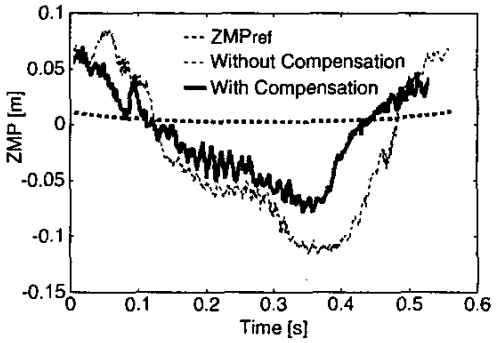

Fig. 9. Trajectiones of ZMP

VI. REFERENCES

[1] M. Vukobratovic, et. al., IEEE Trans. on Bio-Mechanical Engineering, Vol. BME-17, No.1, pp.25–36, 1970

[2] S. Kajita and K. Tani, J. of Robotics and Mechatronics, 5, 6, 516–522, 1993

[3] I. Simoyama, Trans. of the Japan Society of Mechanical Engineers, 48, 433, 455–1455, 1982

[4] T. Furuta, Y. Okumura, and K. Tomiyama, IEEE-RAS Int. Conf. on Humanoid Robots, no.84, 2000

[5] K. Hirai, et. al., Proc. of ICRA'98, 1321–1326, 1998

[6] H. Inoue, Proc. IARP Humanoid and Human Friendly Robotics, I-1-1-4, 1998

[7] T. Morita, H. Iwata, and S. Sugano, Proc. of Int. Symposium on Humanoid Robots, 181–186, 1999

[8] J. Furusho and A. Sano , Int. J. of Robotics Research, 9, 2, 83–98, 1990.

[9] M.Yamada, J.Furusho and A.Sano, Proc. of ICAR'85, 405–412, 1985.

[10] H. Minakata and Y. Hori, 4rd Int. Workshop on Advanced Control, 460–467, 1993

[11] T. Furuta et. al, Asian Control Conference, Vol. 2, 515–517, 1997